Electronic Supporting Information (ESI) for the manuscript:

Redox switching of the antiferromagnetic coupling in permethylated dicopper(II) paracyclophanes

Jesús Ferrando-Soria, María Castellano, Rafael Ruiz-García, Joan Cano, Miguel Julve, Francesc Lloret,* Jorge Pasán, Catalina Ruiz-Pérez, Laura Cañadillas-Delgado, Yangling Li, Yves Journaux, and Emilio Pardo*

Table of Contents

Materials

All chemicals were of reagent grade quality. They were purchased from commercial sources and used as received, except those for electrochemical measurements. The nBu$_4$NPF$_6$ salt was recrystallized twice from ethyl acetate/diethyl ether, dried at 80 °C under vacuum, and kept in an oven at 110 °C. Acetonitrile was purified by distillation from calcium hydride on activated 3 Å molecular sieves and stored under argon. The *N,N′-p*-phenylenebis(oxamic acid ethyl ester) (Et$_2$H$_2$ppba) proligand and (Ph$_4$P)$_4$[Cu$_2$(ppba)$_2$] · 8H$_2$O (**1a**) were prepared by literature methods.[1]

Physical techniques

Elemental analyses (C, H, N) were performed at the Servicio Central de Soporte a la Investigación (SCSIE) at the Universitat de València (Spain). ^{1}H NMR spectra were recorded at room temperature on a Bruker AC 200 (200.1 MHz) spectrometer. Chemical shifts are reported in δ (ppm) *vs*. TMS. C$_2$D$_6$SO was used as solvent and internal standard (δ = 2.50 ppm). FTIR spectra were recorded on a Nicolet-5700 spectrophotometer as KBr pellets.

1 E. Pardo, J. Faus, M. Julve, F. Lloret, M. C. Muñoz, J. Cano, X. Ottenwaelder, Y. Journaux, R. Carrasco, G. Blay, I. Fernández and R. Ruiz-García, *J. Am. Chem. Soc.*, 2003, **125**, 10770.

Preparation of the ligands

The 2-methyl-*N,N'*-*p*-phenylenebis(oxamic acid ethyl ester) ($Et_2H_2Meppba$) and 2,3,5,6-tetramethyl-*N,N'*-*p*-phenylenebis(oxamic acid ethyl ester) ($Et_2H_2Me_4ppba$) proligands were synthesized from the straightforward condensation of the corresponding commercially available polymethyl-substituted *p*-phenylenediamine precursors with ethyl oxalyl chloride ester (1:2 molar ratio), as reported previously for the parent Et_2H_2ppba proligand.[1]

$Et_2H_2Meppba$: Ethyl oxalyl chloride ester (14.0 mL, 120 mmol) was poured into a solution of 2-methyl-*p*-phenylenediamine dihydrogen sulfate (13.2 g, 60 mmol) and triethylamine (16.8 mL, 120 mmol) in THF (250 mL) under vigorous stirring at 0 °C on an ice-bath. The reaction mixture was then refluxed for 1 h. After cooling, the solid was collected by filtration, washed thoroughly with water to remove the precipitate of $(Et_3NH)_2SO_4$ and then with diethyl eter, and dried under vacuum (15.5 g, 80% yield). Anal.: calcd for $C_{15}H_{18}N_2O_6$ (322): C, 55.90; H, 5.59; N, 8.70%. Found: C, 55.87; H, 5.29; N, 8.91%; ^{1}H NMR (C_2D_6SO): δ = 1.28 (t, 6 H, 2 CH_3), 2.18 (s, 3H, CH_3 of $C_6H_3CH_3$), 4.23 (q, 4 H, 2 CH_2O), 7.29 (d, 1 H, 5–H of $C_6H_3CH_3$), 7.58 (d, 1 H, 4–H of $C_6H_3CH_3$), 7.63 (s, 1 H, 3–H of $C_6H_3CH_3$), 10.32 (s, 1 H, 1 NH), 10.80 (s, 1 H, 1 NH); IR (KBr): ν = 3399 (N–H), 1732, 1704 cm^{-1} (C=O).

$Et_2H_2Me_4ppba$: Ethyl oxalyl chloride ester (14.0 mL, 120 mmol) was poured into a solution of 2,3,5,6-tetramethyl-*p*-phenylenediamine (9.9 g, 60 mmol) in THF (250 mL) under vigorous stirring at 0 °C on an ice-bath. The reaction mixture was then refluxed for 1 h. After cooling, the solid was collected by filtration, washed with diethyl eter, and dried under vacuum (19.7 g, 90% yield). Anal.: calcd for $C_{18}H_{24}N_2O_6$ (364): C, 59.33; H, 6.64; N, 7.68%. Found: C, 58.98; H, 6.67; N, 7.74%; ^{1}H NMR (C_2D_6SO): δ = 1.34

(t, 6 H, 2 CH_3), 2.02 (s, 12H, 4 CH_3 of $C_6(CH_3)_4$), 4.32 (q, 4 H, 2 CH_2O), 10.43 (s, 2 H, 2 NH); ν = 3245 (N–H), 1728, 1676 cm^{-1} (C=O).

Scheme S1 Synthesis of the Et_2H_2L proligands (L = ppba, Meppba, and Me_4ppba): (a) $C_2O_2Cl(OEt)$, THF; (b) $C_2O_2Cl(OEt)$, Et_3N, THF.

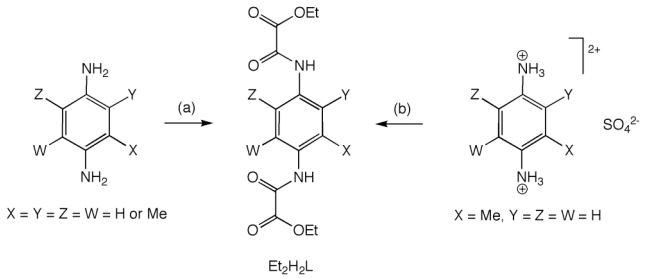

Preparation of the complexes

Complexes **1b** and **1c** were synthesized by two successive steps after metathesis of the corresponding lithium(I) salts with tetraphenylphosphonium chloride in water/acetonitrile via the intermediacy of the silver(I) salts, as reported previously for the parent complex **1a**.[1]

$(Ph_4P)_4[Cu_2(Meppba)_2] \cdot 8H_2O$ (1b): An aqueous solution (10 mL) of $Cu(NO_3)_2 \cdot 3H_2O$ (1.2 g, 5 mmol) was added dropwise to a solution of $Et_2H_2Meppba$ (1.6 g, 5 mmol) and $LiOH \cdot H_2O$ (0.8 g, 20 mmol) in water (50 mL) under stirring at room temperature. The resulting deep green solution was then filtered, and the solvent was reduced under vacuum until a solid appeared. The dark green solid was collected by filtration, washed with acetone and diethyl ether, and dried under vacuum (1.7 g, 85% yield). Anal.: calcd for $C_{22}H_{28}Cu_2Li_4N_4O_{20}$ (822): C, 32.09; H, 3.43; N, 6.80%. Found: C, 31.34; H, 3.20; N, 6.89%; IR (KBr): ν = 3460 (O–H), 1645, 1618 cm^{-1} (C=O).

An aqueous solution (10 mL) of $AgNO_3$ (1.4 g, 8 mmol) was added to a solution of $Li_4[Cu_2(Meppba)_2] \cdot 8H_2O$ (1.6 g, 2 mmol) in water (20 mL) under stirring at room temperature. The dark brown solid that appeared was collected by filtration, suspended in water (10 mL), and then charged with a solution of Ph_4PCl (3.0 g, 8 mmol) in acetonitrile (5 mL). The reaction mixture was further stirred for 30 min under gentle warming and then filtered to remove the precipitate of AgCl. Small dark brown crystals of **1b** not-suitable for X-ray diffraction were obtained by slow evaporation of the filtered solution after several days in the open air at room temperature (3.9 g, 90% yield). Anal.: calcd for $C_{118}H_{108}Cu_2N_4O_{20}P_4$ (2151): C, 65.82; H, 5.06; N, 2.60%. Found: C, 65.45; H, 4.99; N, 2.77%; IR (KBr): ν = 3425 (O–H), 1642, 1617 cm^{-1} (C=O).

$(Ph_4P)_4[Cu_2(Me_4ppba)_2] \cdot 15H_2O$ (1c): An aqueous solution (10 mL) of $Cu(NO_3)_2 \cdot 3H_2O$ (1.2 g, 5 mmol) was added dropwise to a solution of $Et_2H_2Me_4ppba$ (1.8 g, 5 mmol) and $LiOH \cdot H_2O$ (0.8 g, 20 mmol) in water (50 mL) under stirring at room temperature. The resulting deep brown solution was then filtered, and the solvent was reduced under vacuum until a solid appeared. The dark brown solid was collected by filtration, washed with acetone and diethyl ether, and dried under vacuum (2.0 g, 85% yield). Anal.: calcd for $C_{28}H_{42}Cu_2Li_4N_4O_{21}$ (924): C, 36.34; H, 4.57; N, 6.05%. Found: C, 36.63; H, 4.40; N, 6.03%; IR (KBr): ν = 3473 (O–H), 1634, 1605 cm^{-1} (C=O).

An aqueous solution (10 mL) of $AgNO_3$ (1.4 g, 8 mmol) was added to a solution of $Li_4[Cu_2(Me_4ppba)_2] \cdot 9H_2O$ (1.9 g, 2 mmol) in water (20 mL) under stirring at room temperature. The dark brown solid that appeared was collected by filtration, suspended in water (10 mL), and then charged with a solution of Ph_4PCl (3.0 g, 8 mmol) in acetonitrile (5 mL). The reaction mixture was further stirred for 30 min under gentle warming and then filtered to remove the precipitate of AgCl. X-ray quality dark brown prisms of **1c** were obtained by slow evaporation of the filtered solution after several days in the open air at room temperature (4.2 g, 90% yield). Anal.: calcd for $C_{124}H_{134}Cu_2N_4O_{27}P_4$ (2363): C, 63.02; H, 5.71; N, 2.37%. Found: C, 63.99; H, 5.59; N, 2.46%; IR (KBr): ν = 3413 (O–H), 1637, 1604 cm^{-1} (C=O).

Scheme S2 Synthesis of the complexes $(Ph_4P)_4[Cu_2L_2] \cdot xH_2O$ [L = ppba (1), Meppba (2), and Me_4ppba (3)]: (a) $LiOH \cdot H_2O$, H_2O; (b) $Cu(NO_3)_2 \cdot 3H_2O$, H_2O; (c) $AgNO_3$, H_2O; (d) Ph_4PCl, H_2O/CH_3CN.

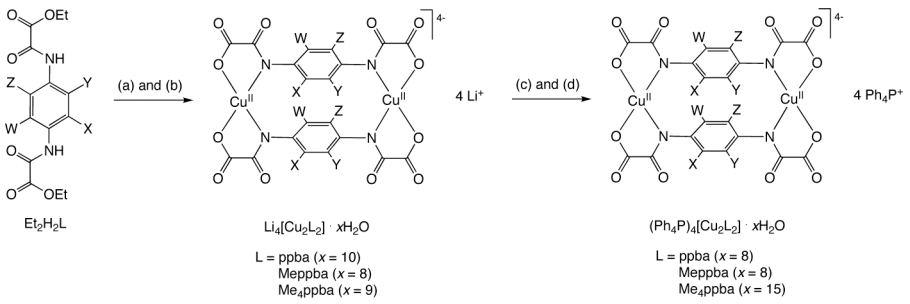

X-ray crystallographic data collection and structure refinement

The X-ray diffraction data of **1c** were collected using synchrotron radiation (λ = 0.7513 Å) at the BM16-CRG beamline in the ESRF (Grenoble, France). The data were indexed, integrated and scaled using the *HKL2000* program.[2] All calculations for data reduction, structure solution, and refinement were done by standard procedures (*WINGX*).[3] The structure of **1c** was solved by direct methods and refined with full-matrix least-squares technique on F^2 using the *SHELXS-97* and *SHELXL-97* programs.[4] The hydrogen atoms from the organic ligands were calculated and refined with isotropic thermal parameters. The final geometrical calculations and the graphical manipulations were carried out with *PARST97* and *CRYSTAL MAKER* programs, respectively.[5] Crystallographic data (excluding structure factors) for the structure reported in this paper have been deposited with the Cambridge Crystallographic Data Centre as supplementary publication numbers CCDC–856597. Copies of the data can be obtained free of charge on application to CCDC, 12 Union Road, Cambridge CB21EZ, UK [fax: (+44) 1223−336−033; e-mail: deposit@ccdc.cam.ac.uk].

2 Z. Otwinowski and W. Minor, *Processing of X-ray Diffraction Data Collected in Oscillation Mode, in Methods in Enzymology: Macromolecular Crystallography*, Part A, Vol. 276 (Eds.: C. W. Jr., Carter and R. M. Sweet), 1997, p. 307.

3 L. J. Farrugia, *J. Appl. Crystallogr*., 1999, **32**, 837 (*WINGX*).

4 G. M. Sheldrick, *SHELX97*, *Programs for Crystal Structure Analysis, release 97-2*, Institüt für Anorganische Chemie der Universität Göttingen, Göttingen, 1998.

5 (*a*) M. Nardelli, *J. Appl. Crystallogr.,* 1995, **28**, 659; (*b*) D. Palmer, *CRYSTAL MAKER,* Cambridge University Technical Services, Cambridge, 1996.

Table S1 Summary of crystallographic data for **1c**

Formula	$C_{124}H_{134}Cu_2N_4O_{27}P_4$
M / g mol^{-1}	2363.31
Crystal system	triclinic
Space group	P–1
a / Å	13.5320(10)
b / Å	15.7080(10)
c / Å	15.8360(10)
α / °	71.2170(10)
β / °	70.9200(10)
γ / °	68.9650(10)
V / Å^3	2888.2(3)
Z	1
ρ_{calc} / g cm^{-3}	1.359
μ / mm^{-1}	0.501
T / K	100(2)
Reflect. collcd.	9167
Reflect. obs. [$I > 2\sigma(I)$]	9045
Data / restraints / parameters	9045 / 0 / 735
R_1[a] [$I > 2\sigma(I)$] (all)	0.0412 (0.0415)
wR_2[b] [$I > 2\sigma(I)$] (all)	0.1104 (0.1107)
S[c]	1.036

[a] $R_1 = \sum(|F_o| - |F_c|)/\sum|F_o|$. [b] $wR_2 = [\sum w(F_o^2 - F_c^2)^2/\sum w(F_o^2)^2]^{1/2}$. [c] $S = [\sum w(|F_o| - |F_c|)^2/(N_o - N_p)]^{1/2}$.

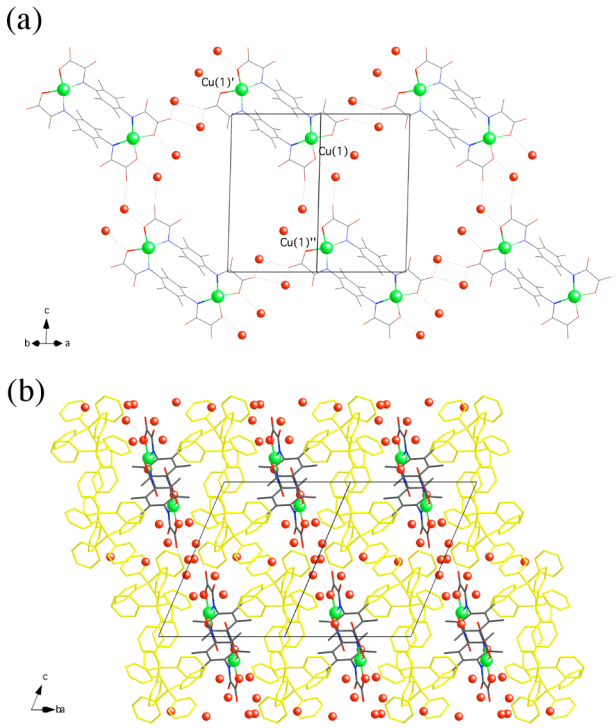

Fig. S1 (a) Projection view of a layer of hydrogen-bonded anionic dicopper units of **1c** along the [110] direction [symmetry code: (I) = 2 – x, 1 – y, – z; (II) = 1 – x, 1 – y, 1 – z]. The hydrogen bonds are represented by dotted lines. (b) Crystal packing view of **1c** along the [–110] direction. The tetraphenylphosphonium cations are shown in yellow color (hydrogen atoms have been omitted for clarity).

Magnetic measurements

Variable-temperature (2.0–300 K) magnetic susceptibility measurements were carried out with a SQUID magnetometer under an applied field of 10 kOe ($T \geq 50$ K) and 100 Oe ($T < 50$ K). The experimental data were corrected for the diamagnetic contributions of the constituent atoms and the sample holder as well as for the temperature-independent paramagnetism (tip) of the Cu^{II} ion (60×10^{-6} cm^3 mol^{-1}).

Table S2 Selected magnetic data for **1a**–**c**

Complex	J^a / cm^{-1}	g^a	$R^b \times 10^5$
1a	–94	2.06	6.9
1b	–124	2.10	4.0
1c	–144	2.08	2.7

[a] The magnetic coupling parameter (J) and the Landé factor (g) in the spin Hamiltonian $\mathbf{H} = -J\,\mathbf{S_1} \cdot \mathbf{S_2} + g\beta H(\mathbf{S_1} + \mathbf{S_2})$ (with $S_1 = S_2 = S_{Cu} = 1/2$) were obtained by least-squares fit of the experimental data through the Bleaney-Bowers expression, $\chi_M = (2N\beta^2g^2/k_BT) / [3 + \exp(-J/k_BT)]$ (where N is the Avogadro number, β is the Bohr magneton, and k_B is the Boltzmann constant). [b] The agreement factor is defined as $R = \sum[(\chi_M T)_{exp} - (\chi_M T)_{calcd}]^2/\sum[(\chi_M T)_{exp}]^2$

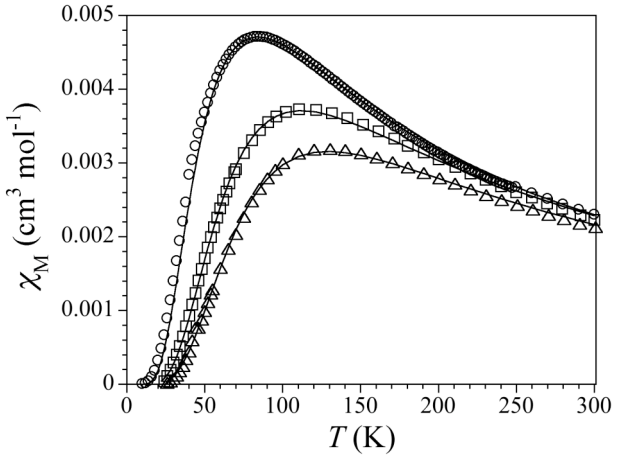

Fig. S2 Temperature dependence of χ_M for **1a** (○), **1b** (□), and **1c** (△). The solid lines are the best-fit curves (data from Table S2).

Electrochemical measurements

The electrochemical studies were performed using a PAR 273A scanning potentiostat operating at a scan rate of 10–1000 mV s^{-1}. Cyclic voltammograms were carried out in acetonitrile using 0.1 M nBu$_4$NPF$_6$ as supporting electrolyte and 1.0 mM of **1a**–**c**. The working electrode was a glassy carbon disk (0.32 cm^2) that was polished with 1.0 μm diamond powder, sonicated, washed with absolute ethanol and acetone and air dried. The reference electrode was $AgClO_4$/Ag separated from the test solution by a salt bridge containing the solvent/supporting electrolyte, with platinum as auxiliary electrode. All experiments were performed in standard electrochemical cells at 25 °C under argon. The potential range investigated was between –2.00 and +1.80 V *vs*. SCE. The formal potentials were measured at a scan rate of 100 mV s^{-1} and were referred to the saturated calomel electrode (SCE), which was consistently measured as –0.26 V *vs*. the $AgClO_4$/Ag electrode. Ferrocene was added as internal standard at the end of the measurements [$E(Fc^+/Fc)$ = +0.40 V *vs*. SCE]. The values of the anodic peak to cathodic peak separation of the first redox wave for **1a**–**c** are comparable to that of the ferricinium/ferrocene couple [ΔE = 70 mV]. A perfect linear plot of the peak current against the square root of the scan rate is obtained for the first redox wave of **1c**, which is then stated to be completely reversible on the voltammetric time-scale.

Table S3 Selected electrochemical[a] data for **1a**–**c**

Complex	E_1^b / V	E_2^b / V	K_c^c
1a	+0.33 (80)	+0.79 (i)	0.6×10^8
1b	+0.24 (80)	+0.80 (i)	0.3×10^{10}
1c	+0.15 (70)	+0.86 (i)	1.1×10^{12}

[a] In acetonitrile (25 °C, 0.1 M nBu$_4$NPF$_6$) with a scan rate of 100 mV s^{-1}. [b] All formal potential (E) values were taken as the half-wave potentials *vs*. SCE, except for the irreversible (i) waves for which the anodic peak potentials were given. The values of the peak-to-peak separation (ΔE / mV) between the anodic and cathodic peak potentials are given in parentheses. [c] The values of the comproportionation constant (K_c) were estimated from the difference in the formal potential values between the two one-electron oxidation waves ($\Delta E_{12} = E_2 - E_1$) through the expression $\log K_c = \Delta E_{12}/0.059$.

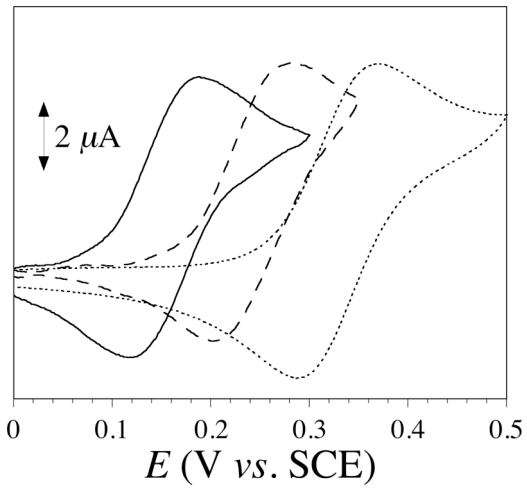

Fig. S3 CVs of **1a** (dotted line), **1b** (dashed line), and **1c** (solid line) in acetonitrile at 25 °C (0.1 M nBu$_4$NPF$_6$) with a scan rate of 100 mV s^{-1}.

Chemical oxidation procedures and spectroscopic measurements

Varying amounts of a 0.01 M solution of bromine (0–15 μL) were added stepwise to a 0.1 mM solution of **1c** in acetonitrile (2.5 mL) at different temperatures in the range of 5–25 °C. UV–vis–NIR solution spectra were recorded on an Agilent Technologies-8453 spectrophotometer equipped with a thermostated Chem Station. The course of the decomposition reaction of **2c** was followed by measuring the absorbance at λ_{max} = 875 nm as a function of time.

The monooxidized species **2c** was obtained by addition of an excess of Br_2 to a 0.1 M solution of **1c** in acetonitrile at –40 °C. Variable-temperature (4.0–150 K) X-band EPR spectra (ν = 9.47 GHz) of frozen-matrix acetonitrile solutions of **1c** and **2c** were recorded under non-saturating conditions on a Bruker ER 200 D spectrometer equipped with a helium cryostat. The simulated EPR spectra were obtained by using the *XSOPHE* program.[6]

6 G. R. Hanson, K. E. Gates, C. J. Noble, M. Griffin, A. Mitchell and S. Benson, *J. Inorg. Biochem*., 2004, **98**, 903 (*XSOPHE*).

Table S4 Selected kinetic[a] data for the decomposition of **2c**

T / °C	c_0[b] × 10^4 / M	k[b] / M^{-1} s^{-1}	$t_{1/2}$[c] / h
5	1.00(1)	0.295(3)	9.4
15	0.64(2)	0.598(6)	7.3
25	0.48(4)	1.86(2)	3.1

[a] In acetonitrile. [b] The initial concentration (c_0) and the second-order rate constant (k) values were calculated from the reciprocal of the absorbance at λ_{max} = 875 nm ($1/A_{875}$) *vs.* time (t) plots through the expression $(1/c) = (1/c_0) + kt$ with $c = A_{875}/(l \times \varepsilon_{875})$, where l is the path length (l = 1 cm) and ε_{875} is the molar extinction cofficient at λ_{max} = 875 nm (ε_{875} = 5660 M^{-1} cm^{-1}). [c] The half-life ($t_{1/2}$) is the time required for the concentration to fall from c_0 to $c_0/2$ [$t_{1/2} = (1/c_0)(1/k)$].

Table S5 Selected UV–Vis–NIR[a] and EPR[b] spectral data for **1c** and **2c**

Complex	λ_{max}[c] / nm	ε[d] / M^{-1} cm^{-1}	g_x[e]	A_x[e] / G	g_y[e]	A_y[e] / G	g_z[e]	A_z[e] / G
1c	325 (30770)	6450	2.005	20 (0.0019)	2.085	15 (0.0015)	2.239	93 (0.0097)
	420 (23810)	3810						
2c	595 (16805)	1460	2.012	30 (0.0028)	2.065	20 (0.0019)	2.250	108 (0.0113)
	875 (11430)	5660						

[a] In acetonitrile at 5 °C. [b] In acetonitrile at 77 (**1c**) and 4 K (**2c**). [c] The calculated values of the wavenumber ($\nu = 1/\lambda_{max}$) in cm^{-1} units are given in parentheses. [d] Molar extinction cofficient. [e] The values of the Landé factors (g_i) and the hyperfine coupling constants (A_i) associated with the x, y, and z components of the allowed $M_s = 0 \rightarrow M_s = \pm 1$ transitions of the excited triplet (S = 1) spin state for **1c**, and the corresponding ones of the $M_s = -1/2 \rightarrow M_s = +1/2$ transition of the ground doublet (S = 1/2) spin state for **2c** were calculated by using the *XSOPHE* program. The calculated A_i values in cm^{-1} units are given in parentheses.

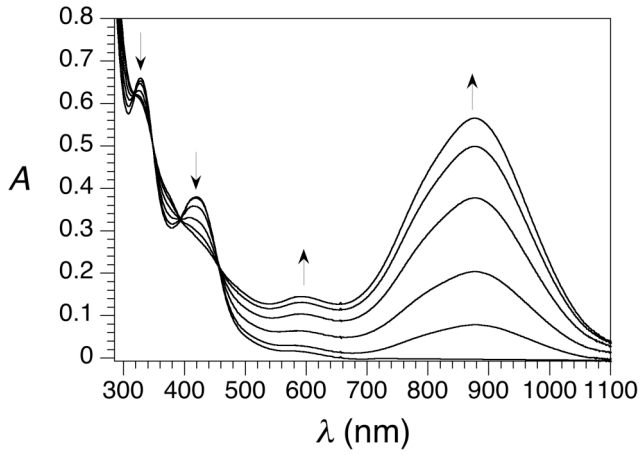

Fig. S4 UV–Vis–NIR spectral changes for the chemical oxidation of **1c** with Br_2 in acetonitrile at 5 ˚C. The arrows indicate the course of the reaction.

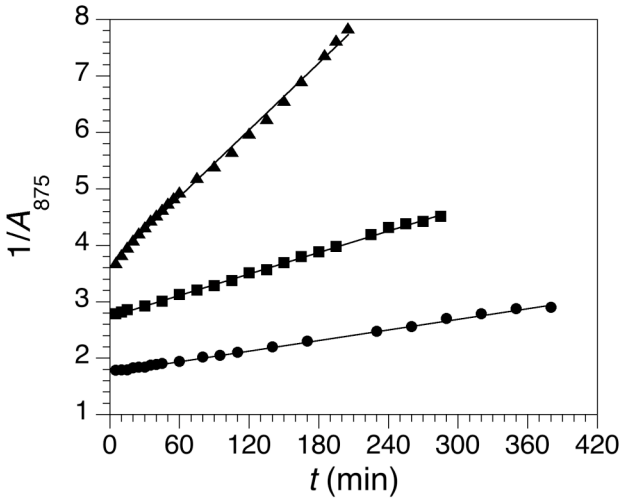

Fig. S5 Time evolution of the reciprocal of the absorbance at λ_{max} = 875 nm ($1/A_{875}$) for the decomposition of **2c** in acetonitrile at 5 (●), 15 (■), and 25 ˚C (▲). The solid lines correspond to the bes-fit curves (data from Table S4).

(a)

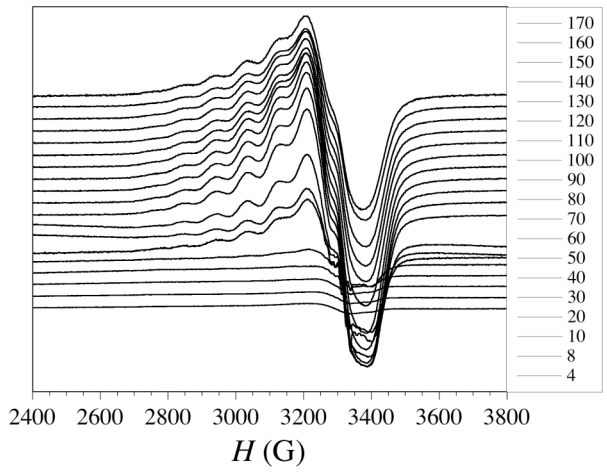

(b)

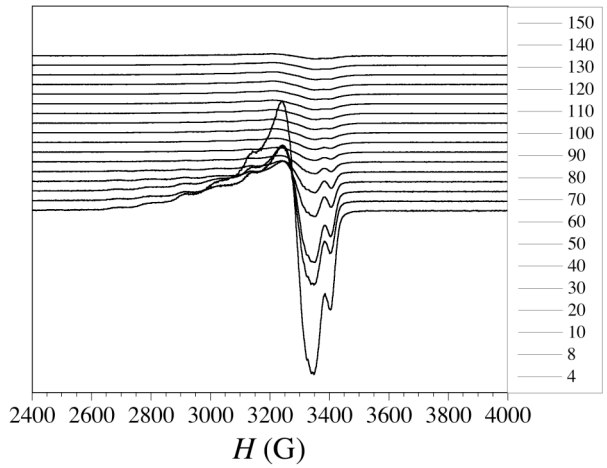

Fig. S6 Temperature dependence of the X-band EPR spectra of **1c** (a) and **2c** (b) in acetonitrile.

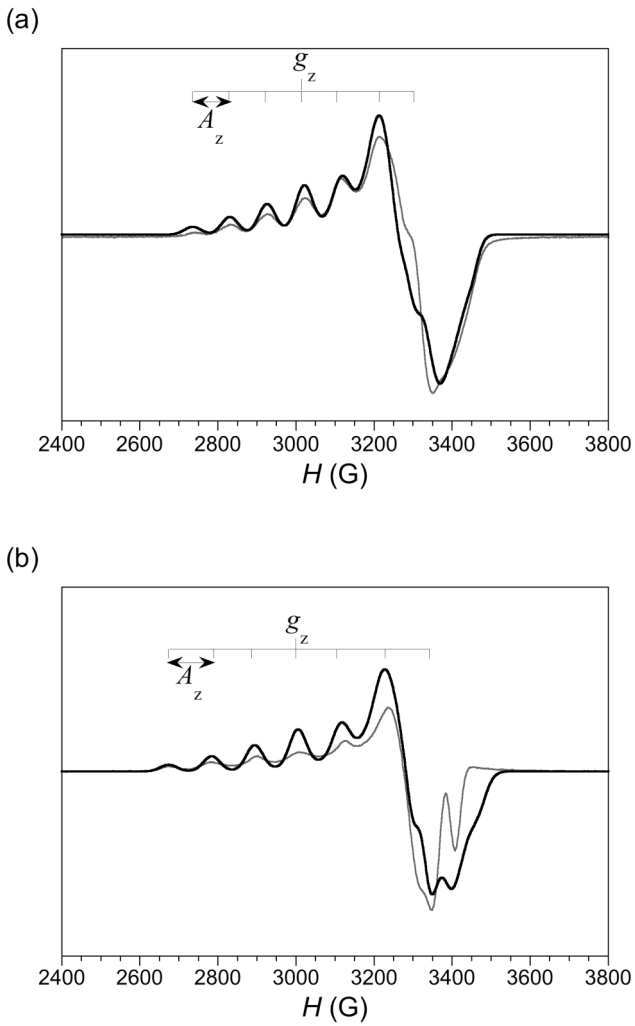

Fig. S7 X-band EPR spectra of **1c** (a) and **2c** (b) at 77 and 4 K respectively, in acetonitrile. The bold lines are the simulated spectra (data from Table S5).

Computational details

Density functional (DF) calculations were carried out on the optimized molecular geometries of **1a–c** in acetonitrile solution using the hybrid B3LYP method[7] combined with the broken-symmetry (BS) approach,[8] as implemented in the Gaussian 09 program.[9] Solvation effects were introduced using a polarizable continuum model (PCM), where the cavity is created via a series of overlapping spheres.[10] Triple- and double-ζ quality basis sets proposed by Ahlrichs and co-workers were used for the metal and non-metal atoms, respectively.[11] The calculated spin density data for **1c** and **2c** were obtained from natural bond orbital (NBO) analysis.[12]

Different ground electronic configurations are available for the oxidized species **2c** depending on the oxidized center (metal or organic ligand) and the overall spin state (doublet or quartet). In the geometry optimization process, a unique result was found in all cases even if the starting geometry was modified in each case to come closer to those experimentally observed in either copper(III) complexes or radical ligands. In fact, the $S = 1/2$ Cu^{II}_2-π-radical configuration is the most stable one and

7 A. D. Becke, *J. Chem. Phys.,* 1993, **98**, 5648.

8 (*a*) E. Ruiz, J. Cano, S. Alvarez and P. Alemany, *J. Comput. Chem.,* 1999, **20**, 1391; (*b*) E. Ruiz, A. Rodriguez-Fortea, J. Cano, S. Alvarez and P. Alemany, *J. Comput. Chem.,* 2003, **24**, 982.

9 M. J. Frisch, G. W. Trucks, H. B. Schlegel, G. E. Scuseria, M. A. Robb, J. R. Cheeseman, G. Scalmani, V. Barone, B. Mennucci, G. A. Petersson, H. Nakatsuji, M. Caricato, X. Li, H. P. Hratchian, A. F. Izmaylov, J. Bloino, G. Zheng, J. L. Sonnenberg, M. Hada, M. Ehara, K. Toyota, R. Fukuda, J. Hasegawa, M. Ishida, T. Nakajima, Y. Honda, O. Kitao, H. Nakai, T. Vreven, J. A. Montgomery, Jr., J. E. Peralta, F. Ogliaro, M. Bearpark, J. J. Heyd, E. Brothers, K. N. Kudin, V. N. Staroverov, R. Kobayashi, J. Normand, K. Raghavachari, A. Rendell, J. C. Burant, S. S. Iyengar, J. Tomasi, M. Cossi, N. Rega, J. M. Millam, M. Klene, J. E. Knox, J. B. Cross, V. Bakken, C. Adamo, J. Jaramillo, R. Gomperts, R. E. Stratmann, O. Yazyev, A. J. Austin, R. Cammi, C. Pomelli, J. W. Ochterski, R. L. Martin, K. Morokuma, V. G. Zakrzewski, G. A. Voth, P. Salvador, J. J. Dannenberg, S. Dapprich, A. D. Daniels, Ö. Farkas, J. B. Foresman, J. V. Ortiz, J. Cioslowski and D. J. Fox, *Gaussian 09, Revision A.1*, Gaussian, Inc., Wallingford CT, 2009.

10 (*a*) M. Cossi, N. Rega, G. Scalmani and V. Barone, *J. Comp. Chem.,* 2003, **24**, 669; (*b*) J. Tomasi, B. Mennucci and E. Cances, *J. Mol. Struct.-Theochem.,* 1999, **464**, 211.

11 (*a*) A. Schaefer, H. Horn and R. Ahlrichs, *J. Chem. Phys.,* 1992, **97**, 2571; (*b*) A. Schaefer, C. Huber and R. Ahlrichs, *J. Chem. Phys.,* 1994, **100**, 5829.

12 (*a*) J. E. Carpenter and F. Weinhold, *J. Mol. Struct.,* 1988, **169**, 41; (*b*) A. E. Reed, L. A. Curtis and F. Weinhold, *Chem. Rev.,* 1988, **88**, 899; (*c*) F. Weinhold and J. E. Carpenter, *The Structure of Small Molecules and Ions*, Plenum, 1988, p 227.

moreover, there is no energy barrier with other possible electronic configurations.

Table S6. Selected atomic spin density data for the optimized geometries in acetonitrile solution of the ground BS singlet and doublet spin states of **1c** and **2c**, respectively[a,b]

	1c	**2c**
Cu(1)	±0.5553	+0.4915
N(1)	–0.1027	+0.0390
N(2)	+0.1021	+0.0389
O(1)	–0.0947	+0.0815
O(2)	–0.0078	+0.0086
O(3)	–0.0068	–0.0017
O(4)	+0.0946	+0.0813
O(5)	+0.0077	+0.0086
O(6)	+0.0067	–0.0018
C(1)	+0.0401	–0.1121
C(2)	–0.0346	+0.0039
C(3)	+0.0345	+0.0037
C(4)	–0.0401	–0.1121
C(5)	+0.0344	–0.0027
C(6)	–0.0343	–0.0030
C(7)	+0.0026	–0.0045
C(8)	+0.0067	–0.0055
C(9)	–0.0025	–0.0045
C(10)	–0.0068	–0.0055
C(20)	+0.0026	+0.0006
C(30)	–0.0025	+0.0006
C(50)	–0.0025	+0.0017
C(60)	+0.0025	+0.0017

[a] The calculated values of the atomic spin density (ρ_X) are given in e units.
[b] The atom-numbering scheme is given in Fig. 1a.